

Arylazopyrazoles for Long-Term Thermal Energy Storage and Optically-Triggered Heat Release below 0 °C

Mihael A. Gerkman, Rosina S. L. Gibson, Joaquín Calbo, Yuran Shi, Matthew J Fuchter, and Grace G. D. Han

J. Am. Chem. Soc., **Just Accepted Manuscript** • DOI: 10.1021/jacs.0c00374 • Publication Date (Web): 22 Apr 2020

Downloaded from pubs.acs.org on April 22, 2020

Just Accepted

“Just Accepted” manuscripts have been peer-reviewed and accepted for publication. They are posted online prior to technical editing, formatting for publication and author proofing. The American Chemical Society provides “Just Accepted” as a service to the research community to expedite the dissemination of scientific material as soon as possible after acceptance. “Just Accepted” manuscripts appear in full in PDF format accompanied by an HTML abstract. “Just Accepted” manuscripts have been fully peer reviewed, but should not be considered the official version of record. They are citable by the Digital Object Identifier (DOI®). “Just Accepted” is an optional service offered to authors. Therefore, the “Just Accepted” Web site may not include all articles that will be published in the journal. After a manuscript is technically edited and formatted, it will be removed from the “Just Accepted” Web site and published as an ASAP article. Note that technical editing may introduce minor changes to the manuscript text and/or graphics which could affect content, and all legal disclaimers and ethical guidelines that apply to the journal pertain. ACS cannot be held responsible for errors or consequences arising from the use of information contained in these “Just Accepted” manuscripts.

Arylazopyrazoles for Long-Term Thermal Energy Storage and Optically-Triggered Heat Release below 0 °C

Mihael A. Gerkman^{1†}, Rosina S. L. Gibson^{2†}, Joaquín Calbo³, Yuran Shi¹, Matthew J. Fuchter^{2*}, Grace G. D. Han^{1*}

¹Department of Chemistry, Brandeis University, 415 South Street, Waltham, MA 02453, USA

²Molecular Sciences Research Hub, Department of Chemistry, Imperial College London, Wood Lane, London W12 0BZ, United Kingdom

³Instituto de Ciencia Molecular, Universidad de Valencia, 46100 Burjassot, Spain

Keywords: photo-switch, arylazopyrazole, phase transition, heat storage, sub-zero heat release

Supporting Information

ABSTRACT: Arylazopyrazole derivatives based on four core structures (4pzMe, 3pzH, 4pzH, and 4pzH-F₂) and functionalized with a dodecanoate group were demonstrated to store thermal energy in their metastable *Z* isomer liquid phase and release the energy by optically triggered crystallization at -30 °C for the first time. Three heat storage-release schemes were discovered involving different activation methods (optical, thermal, or combined) for generating liquid-state *Z* isomers capable of storing thermal energy. Visible light irradiation induced the selective crystallization of the liquid phase via *Z*-to-*E* isomerization, and the latent heat stored in the liquid *Z* isomers was preserved for longer than two weeks unless optically triggered. Up to 92 kJ/mol of thermal energy was stored in the compounds demonstrating remarkable thermal stability of *Z* isomers at high temperatures and liquid-phase stability at temperatures below 0 °C.

INTRODUCTION

Photo-switching molecular systems including azobenzenes,¹⁻³ norbornadienes,^{4,7} dihydroazulenes,⁸⁻¹¹ and fulvalenediruthenium complexes¹²⁻¹⁴ have been recognized as molecular solar thermal (MOST) energy storage materials that convert photon energy to thermal energy by reversible isomerization and energy storage in a metastable isomeric state. This class of molecules complements traditional and emerging photothermal materials which directly convert photon energy into heat, for example, from sunlight to significant thermal energy for vaporizing water, despite the lack of the energy storage capability.¹⁵ Among the photo-switching molecular systems listed, azobenzene derivatives have been particularly well explored as MOST compounds due to a plethora of functionalization methods¹⁶⁻¹⁷ available and their remarkable *E*-*Z* isomerization cyclability.¹⁸ Various forms of MOST materials have been developed incorporating azobenzene groups, including small molecules,¹⁹⁻²⁰ oligomers,²¹⁻²² polymers,²³⁻²⁴ carbon nanotubes,²⁵⁻²⁶ and graphene oxides,²⁷⁻²⁸ and have demonstrated energy storage in the metastable *Z* isomer state

upon UV irradiation. One challenge that azobenzene derivatives face as MOST storage materials is their short *Z* isomer half-life ($t_{1/2}$) ranging from seconds to days depending on azobenzene functionalization.²⁹⁻³⁰ The thermal stability of the *Z* isomer is determined by both steric and electronic effects on both the *E*/*Z* ground states and isomerization transition state.^{18, 31} Such thermal stability governs the thermal energy storage lifetime in MOST materials, and various molecular designs have been developed to increase thermal stability of azobenzene *Z* isomers.

One method to increase the half-life of azobenzenes is to replace one of the aryl rings with a pyrazole: the arylazopyrazoles.³²⁻⁴¹ While there are several factors that underpin the increased stability of the azopyrazoles, it is notable that these azo switches have exceptionally long thermal half-lives (days to years). In principle, the increased thermal stability of the *Z* isomer presents a potential for generating MOST materials with elongated total heat storage time and a wider range of temperatures at which heat can be stored. Additionally, arylazopyrazoles can undergo *Z*-*E* isomerization in the presence of protons⁴² and metal ions,⁴³ which opens up the possibility of creating dual-responsive materials that can release heat when exposed to chemical stimuli as well as light.

In addition to addressing the stability of *Z* isomers, continuous effort has been made to increase the total heat storage density in MOST compounds, particularly azobenzenes that show low energy density (41 kJ/mol for pristine).⁴⁴ A prominent strategy harvests the latent heat of azobenzene derivatives as well as the *Z*-*E* isomerization energy by optically changing the phase of the molecules during the photo-isomerization process (*i.e.* solid *E* ↔ liquid *Z*).⁴⁵⁻⁴⁸ The azobenzene derivatives have also been used as a dopant in organic phase change materials to manipulate the solid-liquid phase transition of the composite by optical means.⁴⁹ Despite the increased energy storage density in these materials, the heat storage time is still limited to hours due to the thermal reversion of the azobenzene derivatives, even at room temperature.

To maximize the usefulness of MOST materials, it is important to extend beyond the limited range of temperatures at

which optically controlled heat release can occur currently. Most of the reported systems measure heat release at around room temperature, due to the facile *Z*-to-*E* reversion at high temperatures (above 60 °C).⁴⁹ Moreover, triggered heat release at low temperatures, especially below 0 °C, remains a challenge because the *Z* liquid phase crystallizes and uncontrollably loses latent heat storage.⁵⁰ According to a recent review by Wu and co-workers on the melting points of mono- and di-substituted *E* and *Z* azobenzenes, most of the reported *Z* isomers show high crystallinity and melting points in the range of 20–200 °C,⁴⁵ which implies the uncontrolled crystallization of *Z* isomer below room temperature.

Herein, we present molecular design strategies for azo MOST materials that address both thermal stability of the *Z* isomers and the stability of liquid phase *Z* isomers under 0 °C by using dodecanoate-appended arylazopyrazoles. For the first time, we demonstrate the visible-light-triggered crystallization of photo-switches at –30 °C and the heat storage in stable liquid phase of the *Z* isomer for longer than two weeks. The heat release at such low temperatures has significant implications in de-frosting of engine oils and mechanical parts, and personal heating under extreme cold conditions where other traditional heat generation, such as combustion, is limited.

RESULTS AND DISCUSSION

Structural Design.

Figure 1 shows previous examples of (a, b) azobenzene,^{46, 49, 51–53} and (c) arylazopyrazole⁵⁰ derivatives that are reported to undergo photo-triggered crystallization from a liquid *Z* state to a

solid *E* state for thermal energy release applications. The azobenzene derivative (a) reported by Grossman and coworkers^{49, 53} was integrated with other traditional organic phase-change materials such as fatty acids and paraffins to optically regulate the heat storage and release from the phase-change composite materials. Azobenzene derivatives exhibit a short *Z* isomer half-life in both solution and in the condensed phase at room temperature, which limits the long-term storage of latent heat in the *Z* isomer liquid phase. Arylazopyrazoles functionalized with an alkyl or terminal alkenyl ether group on benzene ring were recently reported by Li and coworkers.⁵⁰ This work showed the light-triggered crystallization of *Z* isomers at room temperature, which was enabled by the relatively low melting points of select *Z* isomers (19–37 °C). However, their design still renders the *Z* isomers to be highly crystalline below room temperature, which prevents the liquid-to-solid phase change and *Z*-to-*E* isomerization below room temperature.

In order to achieve the light-triggered phase transition and heat release at extreme cold, we introduce a new functionalization strategy that stabilizes *Z* liquid phase at very low temperatures (–30 °C, for example) while retaining *E* crystalline phase. The arylazopyrazole parent structures (Figure 1, center) previously reported by Fuchter and coworkers were selected for our study.^{33–34} DSC measurements (Figures S1–S3) and photo-switching studies (Figure S4) first revealed that all of the parent compounds **1–4** were unable to release thermal energy via light-triggered crystallization for various reasons. Compounds **1** and **2**, after initial melting and subsequent cooling, could not be optically triggered to crystallize as a result of

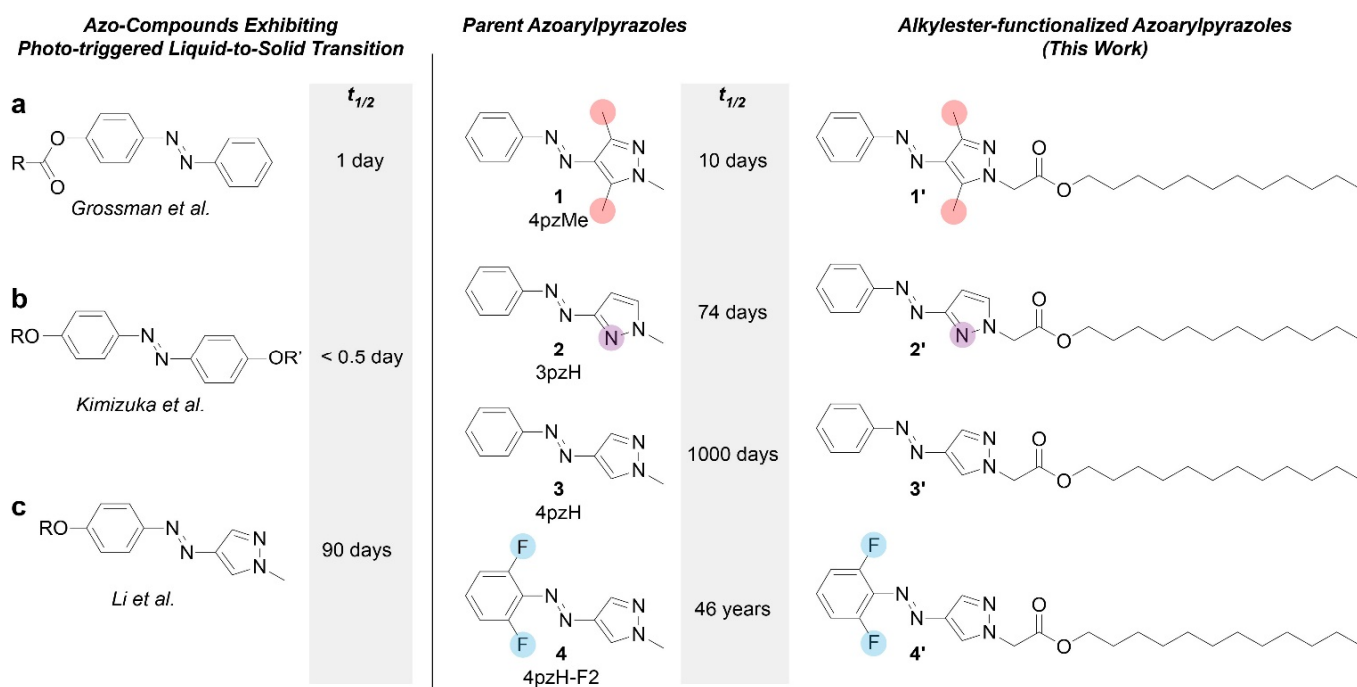


Figure 1. Previous azo-derivatives (azobenzene and arylazopyrazole) that have shown photo-triggered crystallization and heat release. **R** (or **R'**) represents a linear alkyl (Grossman et al.), linear alkyl and oligoether-based ammonium group (Kimizuka et al.), or linear alkyl/terminal alkenyl group (Li et al.). Compounds **1'–4'** are the derivatives of previously synthesized parent azopyrazoles **1–4**, functionalized with dodecanoate group. Thermal *Z* isomer half-lives ($t_{1/2}$) of previous compounds are given in solution at room temperature, except for an azobenzene derivative (Figure 1b) which was measured as a solid. Red, purple, and blue circles show the structural modification from pristine **4pzH** (**3**).

relatively similar thermal characteristics for both isomers. After melting and cooling, they essentially form a stable liquid for both the *E* and *Z* isomeric forms. Compound **4** shows favorable thermal characteristics (*i.e.* liquid *Z* and crystalline *E*, as individually determined by DSC), but the *Z*-to-*E* switching below 39 °C (T_m of *E* form) did not result in any nucleation. Compound **3** shows crystallization by the reverse *E*-to-*Z* photo-isomerization, since the *E* form of compound **3** is less crystalline than its *Z* isomer. However, the photo-induced crystallization did not lead to the overall heat release, because of the larger thermal energy uptake by the isomerization process than the exothermicity from the crystallization. Nonetheless, this intriguing *Z* isomer crystallization is illustrated and discussed in more detail below (schemes compared between Figure 2 and 3) as an alternative new method for potentially storing and releasing thermal energy with reduced activation steps.

The parent arylazopyrazole structures were modified to incorporate a dodecanoate group (**1'**-**4'**). It was hypothesized that such a substituent would increase the crystallinity of *E* isomers *via* the enhanced van der Waals interactions, while producing stable liquid phases for the *Z* isomers. Compounds **1'**-**4'** were particularly designed to preserve the core electronic structure of the parent arylazopyrazoles, with a methylene linker between the alkyl ester group and the photoswitching moiety (Figure 1, right). Comparative UV-Vis spectra of the compounds **1-4** and **1'-4'** (Figure S4) show that light absorption of each parent compound is mostly identical to that of respective alkyl-functionalized derivative. The degrees of *E*-to-*Z* and *Z*-to-*E* photo-isomerizations and the absorption spectra of photo-stationary state (PSS) are essentially unchanged after the functionalization of parent compounds (Table S1). We note that the *E* isomer contents in the photo-irradiated samples are minimal (2-3%) as measured by ¹H NMR (Table S1 and Figure S5).

Phase Transition of Photo-isomers.

The drastic difference in crystallinity between *E* and *Z* forms of our designs was directly measured by differential scanning calorimetry (DSC) as shown in Figure 2b and S1 with a rate of 10 °C/min. The *E* isomers of compounds **1'**-**4'** exhibit sharp melting peaks and subsequent crystallization peaks upon cooling, whereas such melting and crystallization features are absent (compounds **1'**, **3'**, and **4'**) or significantly reduced (compounds **2'**) for the *Z* isomer counterparts. These *Z* isomers were found computationally to have significantly higher polarity than the *E* isomers (Figures S6-S7), which likely contributes to *Z* isomer liquid phase stability upon cooling, along with the increased bulkiness of *Z* isomers. The high polarity and bulkiness of *Z* isomers effectively disrupt the π - π interactions between aromatic groups and van der Waals interactions between the alkyl chains. This disruption reduces the ability of *Z* isomers to pack and form ordered crystals. The alkyl functionalized *Z* isomers were found to remain in the liquid phase either between -45 °C and 85 °C (compounds **1'**, **3'**, and **4'**) or between -30 °C and 10 °C (compound **2'**). Compounds **1'**, **3'**, and **4'** undergo glass transition below -45 °C and *Z*-to-*E* reverse isomerization above 85 °C. Compound **2'** partially crystallizes at temperatures lower than -30 °C and cold-crystallizes at temperatures above 10 °C.

In order to examine the impact of heating and cooling rates on the observed phase transitions, we studied compounds **1'**-

4' at a rate of 1 °C/min by DSC (Figure S2). The *E* isomers of **1'**-**4'** show sharper melting and crystallization peaks, with minimal changes in phase transition temperatures and energies. By running slower measurements, we were able to resolve two crystallization peaks at 32 and 37 °C for the polymorphs of compound **3'**. The *Z* isomer of **1'** exhibits new features including cold crystallization at -4 °C and melting at 47

a I heat & photon absorption (**2'**, **3'**, **4'**)

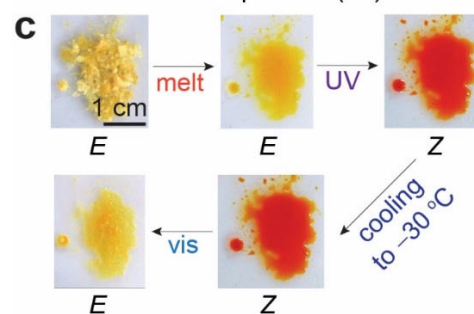
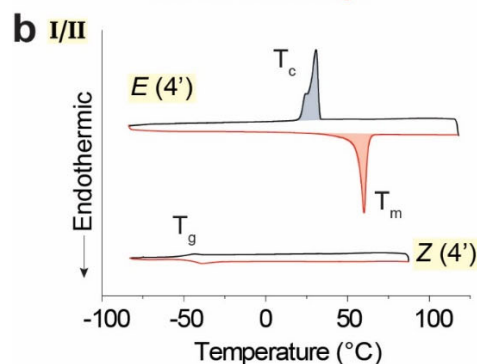
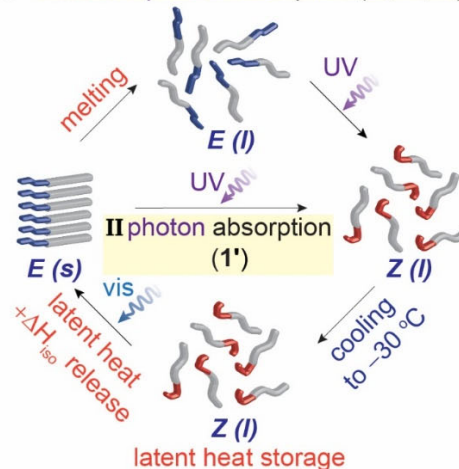


Figure 2. (a) Schematic illustrations of activation methods I and II for arylazopyrazoles derivatives which store latent heat in stable liquid phase upon activation. (b) Differential scanning calorimetry (DSC) plots of *E* and *Z* isomers of compound **4'** as a representative example of group I and II compounds. T_m : melting point, T_c : crystallization point, T_g : glass transition point (c) A series of optical images of compound **1'** in a powder form that undergoes melting, UV irradiation, cooling, and visible-light-induced crystallization according to the activation method I. Compound **1'** also directly absorbs UV at room temperature (*i.e.* in the absence of the first melting process) to form liquid-state *Z* isomer, according to activation method II.

°C, indicating that the prolonged exposure of the amorphous solid to very low temperatures (below -50 °C) generates nucleation seeds which propagates upon thermal activation. The *Z* isomer of **2'** exhibits a broad crystallization around 19 °C instead of cold-crystallization as previously seen at the faster scans. This emphasizes that compound **2'** is more prone to crystallization compared to compounds **1'**, **3'**, and **4'**. We found no impact of scan rate change for the *Z* isomers of **3'** and **4'**.

Regardless of the heating and cooling rate, there is a distinct difference observed between *E* and *Z* isomers of compounds **1'**-**4'**: *E* isomers are highly crystalline while *Z* isomers are liquid at room temperature. This difference between *E* and *Z* forms presents an exciting opportunity for storing latent heat in liquid form and releasing the thermal energy upon photoswitching of the liquid, resulting in crystallization of the photogenerated isomer. For long-term latent heat storage, high *Z* stability of liquid form is required. The arylazopyrazoles, particularly the **4pzH** derived compounds **3** and **4** (and thus **3'** and **4'**), are predicted to retain the *Z* isomer phase for significantly longer periods of time, before being optically triggered to release heat via *Z*-to-*E* isomerization.

Heat Storage and Release Mechanism.

Upon investigation of the mechanisms of latent heat storage and triggered release, three types of energy storage-release cycles were discovered (Figures 2 and 3). Most compounds (**2'**, **3'**, and **4'**) undergo both heat and photon absorption to produce stable liquid phase of *Z* isomers (activation method I). Initially, crystalline *E* isomers absorb heat to become liquid, which in turn absorbs UV photons to isomerize to liquid *Z* isomers. The *Z* liquid-phases are very stable within a wide range of temperatures (-45 °C to $+85$ °C) and can be cooled below 0 °C without losing latent heat. Visible light irradiation isomerizes *Z* back to *E* isomers that readily crystallize even at low temperatures, releasing thermal energy. This process is illustrated visually using compound **1'** in Figure 2c.

In addition to the method previously described (I), compound **1'** can also be activated by an alternative method (II). Method II (Figure 2a) involves the solid-to-liquid phase change upon direct UV irradiation at room temperature. Compound **1'** has the lowest heat of fusion (ΔH_m) in *E* form (Table 1) among the dodecanoate derivatives together with a relatively low melting point (T_m). This suggests that poorer packing of compound **1'** in the solid state enables the direct phase transition upon UV photon uptake. As the *Z* isomers in the stable liquid phase form, compound **1'** can be cooled to low temperatures and optically triggered to release heat, as with compounds **2'**-**4'**.

We note that an intriguing activation method III (Figure 3a) was discovered with parent compound **3** (**4pzH**). This compound shows the opposite thermal behaviors for *E* and *Z* isomers (Figure 3b): the *Z* isomer melts and crystallizes without significant supercooling, similar to the *E* isomers of the other compounds. The *E* isomer of compound **3**, on the other hand, exhibits large supercooling and no crystallization process during cooling to -85 °C. The amorphous solid can then be heated up to 39 °C to recover crystallinity. This cold-crystallization behavior indicates the lack of strong driving force for the molten *E* isomer to crystallize during the cooling cycle. For compound **3**, at a scan rate of 1 °C/min, we observed lowering of

the cold-crystallization temperature of the *E* isomer to -8 °C and minimal change in the *Z* isomer crystallization (Figure S2). The higher crystallinity of the *Z* isomer over the *E* isomer allows for the latent heat storage in the *E* isomer liquid phase and the optical triggering of crystallization by UV-induced *E*-to-*Z* isomerization. The advantage of this activation method (III) is the absence of photon absorption requirement for the generation of the stable liquid phase.

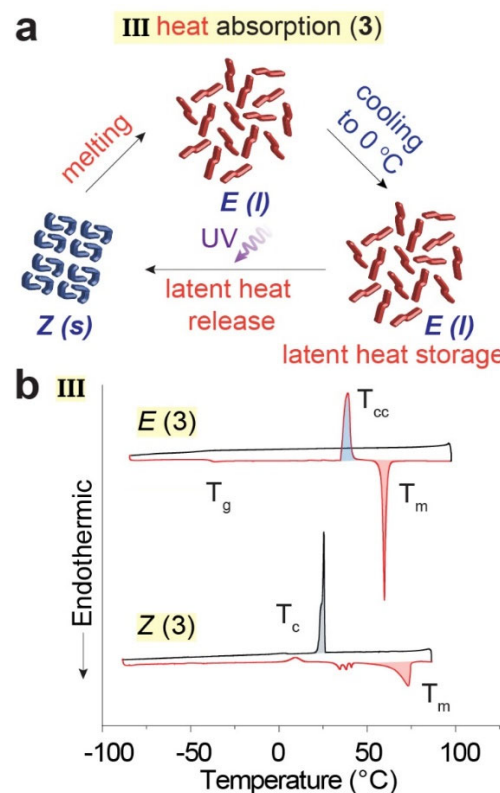


Figure 3. (a) Schematic illustrations of activation method III for arylazopyrazole derivatives which store latent heat in stable liquid phase upon activation. (b) DSC plots of *E* and *Z* isomers of compound **3**, the only group III compound that does not require photon absorption for activation. T_{cc} : cold-crystallization point.

Table 1. Thermal parameters of *E* and *Z* isomers

	<i>E</i>				<i>Z</i>			
	T_m (°C)	ΔH_m (kJ/mol)	T_c (°C)	ΔH_c (kJ/mol)	T_m (°C)	ΔH_m (kJ/mol)	T_c (°C)	ΔH_c (kJ/mol)
1	53	20	22 ^{cc}	17 ^{cc}	94	23	-	-
2	98	21	-5 ^{cc}	15 ^{cc}	56	19	-	-
3	60	21	39 ^{cc}	19 ^{cc}	74	15	23	12
4	96	25	39	22	66	21	16 ^{cc}	15 ^{cc}
1'	67	35	45	35	Liq	Liq	Liq	Liq
2'	91	52	60	49	53	43	-33	7
3'	71	57	28	49	Liq	Liq	Liq	Liq
4'	61	47	30	46	Liq	Liq	Liq	Liq

ΔH_m : heat of fusion, ΔH_c : heat of crystallization, superscript cc: cold-crystallization process. T_c of compounds **1** and **2** *Z* isomers could not be accurately measured due to the concomitant *Z*-to-*E* isomerization during the melting of *Z* isomer and the formation of liquid consisting of *Z* and *E* mixtures.

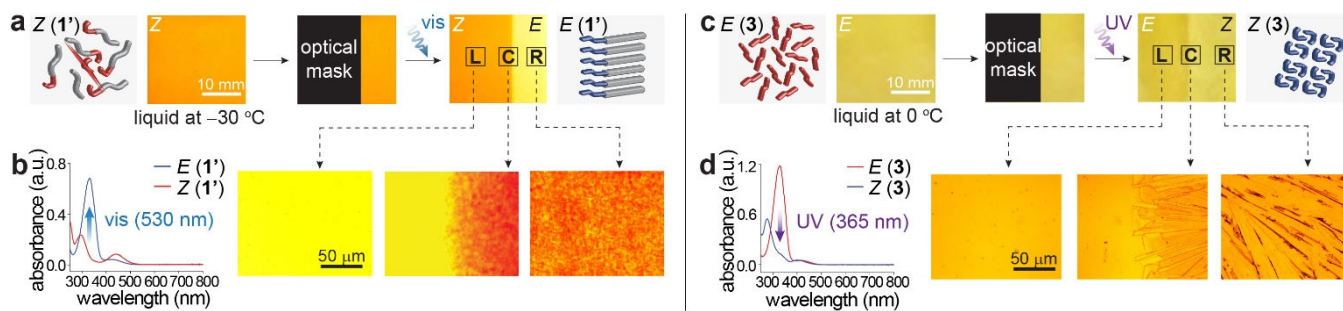


Figure 4. (a) Optical images of a stable liquid film (compound **1'** as an example of group I and II compounds) that is irradiated with visible light (530 nm) at $-30\text{ }^{\circ}\text{C}$ and the subsequent crystallization of *E* isomers. The left side of the film is covered by a mask to preserve *Z* isomers in stable liquid state. Optical microscope images taken on the left (L), center (C), and right (R) spots of the film in (3a), showing liquid phase, interface between liquid and crystalline solid, and solid phase, respectively. (b) UV-Vis absorption spectra of *E* and *Z* forms of compound **1'** obtained in solution. *Z*-to-*E* isomerization is induced by the absorption of 530 nm light by *Z* isomer ($n-\pi^*$ transition). (c) Optical images of a stable liquid film (compound **3** in group III) that is irradiated with UV light (365 nm) at $0\text{ }^{\circ}\text{C}$ and the subsequent crystallization of *Z* isomers. The left side of the film is covered by a mask to preserve *E* isomers in stable liquid state. Optical microscope images taken on a film of compound **3** after selective crystallization by UV irradiation. (d) UV-Vis absorption spectra of *E* and *Z* forms of compound **3** and the process of UV-induced crystallization.

Table 1 summarizes thermal properties of all compounds measured by DSC (Figure S1). The lowest temperature at which thermal energy can be stored in *Z* isomer liquid phase is determined by T_c of *Z* isomers (highlighted red). Compounds **1'**, **3'**, and **4'** in *Z* isomeric forms are confirmed to be liquid above $-45\text{ }^{\circ}\text{C}$, and compound **2'** can preserve liquid phase of *Z* isomers above $-33\text{ }^{\circ}\text{C}$. The highest temperature at which the optical triggering can induce crystallization via *Z*-to-*E* isomerization is defined by T_c of *E* isomers (highlighted blue).

Demonstration of Phase Transition and Heat Release at Low Temperatures.

The temporal and spatial control over latent heat release can be demonstrated by the selective crystallization of stable liquid films involving optical masks (Figure 4). The films were partially covered by the mask (typically thick and dense cardboard or plastic) on the left side (L), and crystalline phase formation was found to occur only within the area (right side, R) exposed to light for 5–15 min. The translucent liquid films become opaque after crystallization (right side, R) observed by darker coloring under optical microscope due to increased diffraction. Compounds **1'**-**4'** (represented in Figure 4a by compound **1'**) show a clear interface between the solid and liquid phase and distinct crystalline features of micro scale grains. Figure 4b shows distinct absorption spectra of *E* and *Z* isomers of compound **1'**, particularly the blue-shifted and diminished $n-\pi^*$ band of *E* isomer in the visible light region, which leads to the prominent color change from orange to yellow upon *Z*-to-*E* isomerization. Comparable data for compounds **2'**-**4'** are provided in the Figure S8. The color change of the compound **3** film (Figure 4c) after irradiation is not as significant as that for compound **1'** (Figure 4a) because of the similar absorption profile and intensity in visible light range (Figure 4d) between *E* and *Z* isomers of compound **3**. Images for compounds **1**, **2**, and **4** are also provided in the Figure S8, demonstrating no crystallization induced by light irradiation. As aforementioned, these compounds remain liquid after *Z*-to-*E* switching due to the high supercooling of melt for both isomers.

DSC was additionally utilized to measure the isomerization energy (ΔH_{iso}) of *Z*-to-*E* switching accompanied by the light-

triggered crystallization (Figure S3). The exothermic peaks appear during the thermal activation of *Z* isomers in DSC, and the integrated area under the peaks represent ΔH_{iso} . As summarized in Table 2, the thermally-induced isomerization occurs at higher temperatures for compounds with higher thermal stability or longer $t_{1/2}$ (T_{iso} of compound **4** > **3** > **2** > **1**; compound **4'** > **3'** > **2'** > **1'**). This indicates the higher thermal activation energy (E_a) of *Z*-to-*E* isomerization for more stable *Z* isomers. ΔH_{iso} , on the other hand, decreases as the *Z* isomer stability is increased (ΔH_{iso} of compounds: **1** > **2** > **3** > **4**; **1'** > **2'** > **3'** > **4'**), indicating the lower energy of the more stable *Z* isomers and corroborating their higher E_a .

Maximum thermal energy release from the optically triggered crystallization process (ΔH_{total}) is calculated by the integration of crystallization energy (ΔH_c) of *E* isomers and *Z*-to-*E* isomerization energy (ΔH_{iso}) for compounds **1'**, **2'**, **3'**, and **4'** following the activation method I and II (marked blue in Table 2). We note that in the case of incomplete *Z*-to-*E* conversion, only a smaller fraction of the ΔH_c and ΔH_{iso} will be harnessed upon optically triggered crystallization. We examined the long-term stability of liquid films at $-20\text{ }^{\circ}\text{C}$ observing no crystallization after two weeks in the case of compounds **3'** and **4'** (Table S2). Compounds **1'** and **2'** were stable for 1 day and 7 hours, respectively, due to the lower *Z* thermal stability (**1'**) and crystallization behavior of *Z* at $-33\text{ }^{\circ}\text{C}$ (**2'**).

We note that compound **3** that is activated by method III results in a negative value of calculated ΔH_{total} due to the endothermic *E*-to-*Z* photo-isomerization required for the crystallization. Since ΔH_{iso} is larger than ΔH_c for compound **3**, the photo-induced crystallization does not lead to the overall heat release. However, this energy storage scheme can be further developed for net heat release by the judicious design of photo-switches that possess small ΔH_{iso} and large ΔH_c . This scheme generates a stable liquid phase without requiring photo-activation and effectively release latent heat by one-step optical triggering. This will potentially open up opportunities to investigate other switches including spiropyrans,⁵⁴ diarylethenes,⁵⁵⁻⁵⁷ or various molecular motors⁵⁸⁻⁶⁰ which have not been considered as MOST molecules due to their negligible ΔH_{iso} . We envision the potential of utilizing photoinduced phase transitions of the aforementioned classes of switches and motors for latent heat storage by careful structural design.

For example, the installation of long alkyl chains can induce crystallinity to materials which can be disrupted by ring opening and closing through photo-irradiation. The substitution pattern of chains on other photo-responsive core structures that would determine the degree of such phase transition is currently under investigation.

Table 2. Thermal Parameters Obtained from DSC

Compound	T_{iso} (°C)	ΔH_{iso} (kJ/mol)	ΔH_{c} (kJ/mol)	ΔH_{total} (kJ/mol)
1	113	49	17	49 ^(a)
2	122	38	12	38 ^(a)
3	155	36	12 ^(b)	-24 ^(c)
4	181	30	22	30 ^(a)
1'	117	47	35	82
2'	137	43	49	92
3'	138	39	49	88
4'	179	31	45	76

ΔH_{total} is the total thermal energy release from the optically triggered crystallization process. T_{iso} is measured as peak temperature of exothermic curve observed for thermally-induced Z-to-E isomerization. (a) $\Delta H_{\text{total}} = \Delta H_{\text{iso}}$ for compounds **1**, **2**, and **4**. (b) ΔH_{c} of compound **3** is the crystallization energy of Z isomers. (c) ΔH_{total} for compound **3** is defined as $\Delta H_{\text{c}} - \Delta H_{\text{iso}}$ due to the endothermic E-to-Z photo-isomerization occurring for the crystallization. DSC plots of Z-to-E thermal isomerization are shown in Figure S3.

CONCLUSION

A series of arylazopyrazole derivatives functionalized with dodecanoate group were demonstrated to be activated thermally, optically, or in combination, to form stable liquid phase Z isomers over a wide range of temperatures. The liquid phase compounds were then optically triggered to isomerize to crystalline forms, releasing latent heat at low temperatures such as -30 °C. The use of an arylazopyrazole core allows for the long-term storage of latent heat in the liquid state, and the dodecanoate group enhances the crystallinity of E isomers while stabilizing the liquid phase of polar Z isomers. This first demonstration of photo-triggered crystallization of molecular switches at temperatures far below 0 °C has significance in applications that require heat release in extreme cold weather that limits ignition of fuels and battery usage. In particular, our molecular system will be able to absorb waste heat from an operating engine and release it later to warm up engine oil when the start is needed at low temperatures (see Supporting Information for detailed description). This waste heat recycling scheme can be applied to other devices that operate intermittently in cold weather, potentially replacing Joule heating (i.e. electrical heating) as conventionally used for such devices. This strategy of molecular designs will be further investigated in other molecular switch systems to improve the energy storage density and to fine-tune the wavelength of light for triggering.

ASSOCIATED CONTENT

Supporting Information

Experimental details, synthesis procedures of compounds **1-4** and **1'-4'**, DSC plots, % of Z isomer measurements, UV-vis

spectra, dipole moment calculations, optical images of films, thin film stability measurement, and NMR spectra supplied as Supporting Information. The Supporting Information is available free of charge via the Internet at <http://pubs.acs.org>. Raw data can be found at 10.14469/hpc/6767.

AUTHOR INFORMATION

Corresponding Author

¹ gracehan@brandeis.edu

² m.fuchter@imperial.ac.uk

Author Contributions

†These authors contributed equally.

Notes

A U.S. provisional patent (62/969,634) was filed on this intellectual property.

ACKNOWLEDGMENT

We acknowledge the SPROUT award (2019-042) from Brandeis Office of Technology Licensing and Provost Research Award from Brandeis University. We thank Prof. Ben Rogers and his laboratory in the Department of Physics at Brandeis University for the usage of optical microscope. R.S.L.G. would like to thank the Faculty of Natural Sciences for the Schrödinger Scholarship. M.J.F. would like to thank the EPSRC for an Established Career Fellowship (EP/R00188X/1).

REFERENCES

1. Fu, L.; Yang, J.; Dong, L.; Yu, H.; Yan, Q.; Zhao, F.; Zhai, F.; Xu, Y.; Dang, Y.; Hu, W.; Feng, Y.; Feng, W. Solar Thermal Storage and Room-Temperature Fast Release Using a Uniform Flexible Azobenzene-Grafted Polynorborene Film Enhanced by Stretching. *Macromolecules* **2019**, *52*, 4222-4231.
2. Wu, S.; Butt, H. J. Solar-Thermal Energy Conversion and Storage Using Photoresponsive Azobenzene-Containing Polymers. *Macromol. Rapid Commun.* **2019**, *41*, 1900413.
3. Zhitomirsky, D.; Cho, E.; Grossman, J. C. Solid-State Solar Thermal Fuels for Heat Release Applications. *Adv. Energy Mater.* **2016**, *6*, 1502006.
4. Lorenz, P.; Hirsch, A. Photoswitchable Norbornadiene-Quadricyclane Interconversion Mediated by Covalently Linked C₆₀. *Chem. Eur. J.* **2020**, *26*, 5220-5230.
5. Mansø, M.; Petersen, A. U.; Wang, Z.; Erhart, P.; Nielsen, M. B.; Moth-Poulsen, K. Molecular Solar Thermal Energy Storage in Photoswitch Oligomers Increases Energy Densities and Storage Times. *Nat. Commun.* **2018**, *9*, 1945.
6. Schuschke, C.; Hohner, C.; Jevric, M.; Ugleholdt Petersen, A.; Wang, Z.; Schwarz, M.; Kettner, M.; Waidhas, F.; Fromm, L.; Sumbly, C. J.; Görling, A.; Brummel, O.; Moth-Poulsen, K.; Libuda, J. Solar Energy Storage at an Atomically Defined Organic-Oxide Hybrid Interface. *Nat. Commun.* **2019**, *10*, 2384.
7. Wang, Z.; Roffey, A.; Losantos, R.; Lennartson, A.; Jevric, M.; Petersen, A. U.; Quant, M.; Dreos, A.; Wen, X.; Sampedro, D.; Börjesson, K.; Moth-Poulsen, K. Macroscopic Heat Release in a Molecular Solar Thermal Energy Storage System. *Energ. Environ. Sci.* **2019**, *12*, 187-193.
8. Broman, S. L.; Nielsen, M. B. Dihydroazulene: from Controlling Photochromism to Molecular Electronics Devices. *Phys. Chem. Chem. Phys.* **2014**, *16*, 21172-21182.
9. Cacciarini, M.; Vlasceanu, A.; Jevric, M.; Nielsen, M. B. An Effective Trigger for Energy Release of Vinylheptafulvene-based Solar Heat Batteries. *Chem. Commun.* **2017**, *53*, 5874-5877.

10. Wang, Z.; Udmark, J.; Börjesson, K.; Rodrigues, R.; Roffey, A.; Abrahamsson, M.; Nielsen, M. B.; Moth-Poulsen, K. Evaluating Di-hydroazulene/Vinylheptafulvene Photoswitches for Solar Energy Storage Applications. *ChemSusChem* **2017**, *10*, 3049-3055.
11. Mogensen, J.; Christensen, O.; Kilde, M. D.; Abildgaard, M.; Metz, L.; Kadziola, A.; Jevric, M.; Mikkelsen, K. V.; Nielsen, M. B. Molecular Solar Thermal Energy Storage Systems with Long Discharge Times Based on the Dihydroazulene/Vinylheptafulvene Couple. *Eur. J. Org. Chem.* **2019**, *2019*, 1986-1993.
12. Moth-Poulsen, K.; Coso, D.; Börjesson, K.; Vinokurov, N.; Meier, S. K.; Majumdar, A.; Vollhardt, K. P. C.; Segalman, R. A. Molecular Solar Thermal (MOST) Energy Storage and Release System. *Environ. Environ. Sci.* **2012**, *5*, 8534-8537.
13. Börjesson, K.; Dzebo, D.; Albinsson, B.; Moth-Poulsen, K. Photon Upconversion Facilitated Molecular Solar Energy Storage. *J. Mater. Chem. A* **2013**, *1*, 8521-8524.
14. Lennartson, A.; Lundin, A.; Börjesson, K.; Gray, V.; Moth-Poulsen, K. Tuning the Photochemical Properties of the Fulvalene-tetracarbonyl-diruthenium System. *Dalton Trans.* **2016**, *45*, 8740-8744.
15. Neumann, O.; Urbam, A. S.; Day, J.; Lal, S.; Nordlander, P.; Halas, N. J. Solar Vapor Generation Enabled by Nanoparticles. *ACS Nano* **2013**, *7*, 42-49.
16. Nguyen, T. H. L.; Gigant, N.; Joseph, D. Advances in Direct Metal-Catalyzed Functionalization of Azobenzenes. *ACS Catal.* **2018**, *8*, 1546-1579.
17. Merino, E. Synthesis of azobenzenes: the coloured pieces of molecular materials. *Chem. Soc. Rev.* **2011**, *40*, 3835-3853.
18. Dong, L.; Feng, Y.; Wang, L.; Feng, W. Azobenzene-based Solar Thermal Fuels: Design, Properties, and Applications. *Chem. Soc. Rev.* **2018**, *47*, 7339-7368.
19. Hu, J.; Huang, S.; Yu, M.; Yu, H. Flexible Solar Thermal Fuel Devices: Composites of Fabric and a Photoliquefiable Azobenzene Derivative. *Adv. Energy Mater.* **2019**, *9*, 1901363.
20. Kunz, A.; Heindl, A. H.; Dreos, A.; Wang, Z.; Moth-Poulsen, K.; Becker, J.; Wegner, H. A. Intermolecular London Dispersion Interactions of Azobenzene Switches for Tuning Molecular Solar Thermal Energy Storage Systems. *ChemPlusChem* **2019**, *84*, 1145-1148.
21. Zhitomirsky, D.; Grossman, J. C. Conformal Electroplating of Azobenzene-Based Solar Thermal Fuels onto Large-Area and Fiber Geometries. *ACS Appl. Mater. Interfaces* **2016**, *8*, 26319-26325.
22. Zhou, H.; Xue, C.; Weis, P.; Suzuki, Y.; Huang, S.; Koynov, K.; Auernhammer, G. K.; Berger, R.; Butt, H.-J.; Wu, S. Photoswitching of Glass Transition Temperatures of Azobenzene-containing Polymers Induces Reversible Solid-to-Liquid Transitions. *Nat. Chem.* **2017**, *9*, 145-151.
23. Saydjari, A. K.; Weis, P.; Wu, S. Spanning the Solar Spectrum: Azopolymer Solar Thermal Fuels for Simultaneous UV and Visible Light Storage. *Adv. Energy Mater.* **2017**, *7*, 1601622.
24. Jeong, S. P.; Renna, L. A.; Boyle, C. J.; Kwak, H. S.; Harder, E.; Damm, W.; Venkataraman, D. High Energy Density in Azobenzene-based Materials for Photo-Thermal Batteries via Controlled Polymer Architecture and Polymer-Solvent Interactions. *Sci. Rep.* **2017**, *7*, 17773.
25. Kucharski, T. J.; Ferralis, N.; Kolpak, A. M.; Zheng, J. O.; Nocera, D. G.; Grossman, J. C. Templated Assembly of Photoswitches Significantly Increases the Energy-Storage Capacity of Solar Thermal Fuels. *Nat. Chem.* **2014**, *6*, 441-447.
26. Jiang, Y.; Huang, J.; Feng, W.; Zhao, X.; Wang, T.; Li, C.; Luo, W. Molecular Regulation of Nano-Structured Solid-State AZO-SWCNTs Assembly Film for the High-Energy and Short-Term Solar Thermal Storage. *Sol. Energy Mater. Sol. Cells* **2019**, *193*, 198-205.
27. Yang, W.; Feng, Y.; Si, Q.; Yan, Q.; Long, P.; Dong, L.; Fu, L.; Feng, W. Efficient Cycling Utilization of Solar-Thermal Energy for Thermochromic Displays with Controllable Heat Output. *J. Mater. Chem. A* **2019**, *7*, 97-106.
28. Pang, W.; Xue, J.; Pang, H. A High Energy Density Azobenzene/Graphene Oxide Hybrid with Weak Nonbonding Interactions for Solar Thermal Storage. *Sci. Rep.* **2019**, *9*, 5224.
29. Olmsted, J.; Lawrence, J.; Yee, G. G. Photochemical Storage Potential of Azobenzenes. *Sol. Energy* **1983**, *30*, 271-274.
30. Asano, T.; Okada, T. Thermal Z-E Isomerization of Azobenzenes. The Pressure, Solvent, and Substituent Effects. *J. Org. Chem.* **1984**, *49*, 4387-4391.
31. Bandara, H. M. D.; Burdette, S. C. Photoisomerization in Different Classes of Azobenzene. *Chem. Soc. Rev.* **2012**, *41*, 1809-1825.
32. Weston, C. E.; Richardson, R. D.; Haycock, P. R.; White, A. J. P.; Fuchter, M. J. Arylazopyrazoles: Azoheteroarene Photoswitches Offering Quantitative Isomerization and Long Thermal Half-Lives. *J. Am. Chem. Soc.* **2014**, *136*, 11878-11881.
33. Calbo, J.; Thawani, A. R.; Gibson, R. S. L.; White, A. J. P.; Fuchter, M. J. A Combinatorial Approach to Improving the Performance of Azoarene Photoswitches. *Beilstein J. Org. Chem.* **2019**, *15*, 2753-2764.
34. Calbo, J.; Weston, C. E.; White, A. J. P.; Rzepa, H. S.; Contreras-García, J.; Fuchter, M. J. Tuning Azoheteroarene Photoswitch Performance through Heteroaryl Design. *J. Am. Chem. Soc.* **2017**, *139*, 1261-1274.
35. Gibson, R. S. L.; Calbo, J.; Fuchter, M. J. Chemical Z-E Isomer Switching of Arylazopyrazoles Using Acid. *ChemPhotoChem* **2019**, *3*, 372-377.
36. Zhang, Z. Y.; He, Y.; Zhou, Y.; Yu, C.; Han, L.; Li, T. Pyrazolylazophenyl Ether-Based Photoswitches: Facile Synthesis, (Near-)Quantitative Photoconversion, Long Thermal Half-Life, Easy Functionalization, and Versatile Applications in Light-Responsive Systems. *Chem. Eur. J.* **2019**, *25*, 13402-13410.
37. Zhang, Y.-M.; Zhang, N.-Y.; Xiao, K.; Yu, Q.; Liu, Y. Photo-Controlled Reversible Microtubule Assembly Mediated by Paclitaxel-Modified Cyclodextrin. *Angew. Chem., Int. Ed.* **2018**, *57*, 8649-8653.
38. Haydell, M. W.; Centola, M.; Adam, V.; Valero, J.; Famulok, M. Temporal and Reversible Control of a DNAzyme by Orthogonal Photoswitching. *J. Am. Chem. Soc.* **2018**, *140*, 16868-16872.
39. Stricker, L.; Fritz, E.-C.; Peterlechner, M.; Doltsinis, N. L.; Ravoo, B. J. Arylazopyrazoles as Light-Responsive Molecular Switches in Cyclodextrin-Based Supramolecular Systems. *J. Am. Chem. Soc.* **2016**, *138*, 4547-4554.
40. Schnurbus, M.; Stricker, L.; Ravoo, B. J.; Braunschweig, B. Smart Air-Water Interfaces with Arylazopyrazole Surfactants and Their Role in Photoresponsive Aqueous Foam. *Langmuir* **2018**, *34*, 6028-6035.
41. Lamping, S.; Stricker, L.; Ravoo, B. J. Responsive Surface Adhesion based on Host-Guest Interaction of Polymer Brushes with Cyclodextrins and Arylazopyrazoles. *Polym. Chem.* **2019**, *10*, 683-690.
42. Gibson, R. S. L.; Calbo, J.; Fuchter, M. J. Chemical Z-E Isomer Switching of Arylazopyrazoles Using Acid. *ChemPhotoChem* **2019**, *3*, 372-377.
43. Hanopolskyi, A. I.; De, S.; Bialek, M. J.; Diskin-Posner, Y.; Avran, L.; Feller, M.; Klajn, R. Reversible Switching of Arylazopyrazole within a Metal-Organic Cage. *Beilstein J. Org. Chem.* **2019**, *15*, 2398-2407.
44. Corruccini, R. J.; Gilbert, E. C. The Heat of Combustion of *cis*- and *trans*-Azobenzene. *J. Am. Chem. Soc.* **1939**, *61*, 2925-2927.
45. Xu, W.-C.; Sun, S.; Wu, S. Photoinduced Reversible Solid-to-Liquid Transitions for Photoswitchable Materials. *Angew. Chem., Int. Ed.* **2019**, *58*, 9712-9740.
46. Ishiba, K.; Morikawa, M. a.; Chikara, C.; Yamada, T.; Iwase, K.; Kawakita, M.; Kimizuka, N. Photoliquefiable Ionic Crystals: A Phase Crossover Approach for Photon Energy Storage Materials with Functional Multiplicity. *Angew. Chem., Int. Ed.* **2015**, *54*, 1532-1536.
47. Han, G. D.; Park, S. S.; Liu, Y.; Zhitomirsky, D.; Cho, E.; Dincă, M.; Grossman, J. C. Photon Energy Storage Materials with High Energy Densities based on Diacetylene-Azobenzene Derivatives. *J. Mater. Chem. A* **2016**, *4*, 16157-16165.
48. Kimizuka, N.; Yanai, N.; Morikawa, M.-a. Photon Upconversion and Molecular Solar Energy Storage by Maximizing the Potential of Molecular Self-Assembly. *Langmuir* **2016**, *32*, 12304-12322.
49. Han, G. G. D.; Deru, J. H.; Cho, E. N.; Grossman, J. C. Optically-Regulated Thermal Energy Storage in Diverse Organic Phase-Change Materials. *Chem. Commun.* **2018**, *54*, 10722-10725.

50. Zhao-Yang, Z.; Tao, L., Efficient Co-Harvesting of Solar Energy and Low-Grade Heat by Molecular Photoswitches for High Energy Density, Long-Term Stable Solar Thermal Battery. *ChemRxiv*. 2019, doi.org/10.26434/chemrxiv.9730694.v1

51. Wang, Z.; Losantos, R.; Sampedro, D.; Morikawa, M.-a.; Börjesson, K.; Kimizuka, N.; Moth-Poulsen, K. Demonstration of an Azobenzene Derivative Based Solar Thermal Energy Storage System. *J. Mater. Chem. A* 2019, 7, 15042-15047.

52. Masutani, K.; Morikawa, M.-a.; Kimizuka, N. A Liquid Azobenzene Derivative as a Solvent-Free Solar Thermal Fuel. *Chem. Commun.* 2014, 50, 15803-15806.

53. Han, G. G. D.; Li, H.; Grossman, J. C. Optically-Controlled Long-Term Storage and Release of Thermal Energy in Phase-Change Materials. *Nat. Commun.* 2017, 8, 1446.

54. Klajn, R. Spiropyran-Based Dynamic Materials. *Chem. Soc. Rev.* 2014, 43, 148-184.

55. Irie, M.; Fukaminato, T.; Matsuda, K.; Kobatake, S. Photochromism of Diarylethene Molecules and Crystals: Memories, Switches, and Actuators. *Chem. Rev.* 2014, 114, 12174-12277.

56. Bléger, D.; Hecht, S. Visible-Light-Activated Molecular Switches. *Angew. Chem., Int. Ed.* 2015, 54, 11338-11349.

57. Boelke, J.; Hecht, S. Designing Molecular Photoswitches for Soft Materials Applications. *Adv. Opt. Mater.* 2019, 7, 1900404.

58. Roke, D.; Sen, M.; Danowski, W.; Wezenberg, S. J.; Feringa, B. L. Visible-Light-Driven Tunable Molecular Motors Based on Oxindole. *J. Am. Chem. Soc.* 2019, 141, 7622-7627.

59. Kassem, S.; van Leeuwen, T.; Lubbe, A. S.; Wilson, M. R.; Feringa, B. L.; Leigh, D. A. Artificial Molecular Motors. *Chem. Soc. Rev.* 2017, 46, 2592-2621.

60. Oruganti, B.; Wang, J.; Durbeej, B. Quantum Chemical Design of Rotary Molecular Motors. *Int. J. Quantum Chem.* 2018, 118, e25405.

